First-principles absorption spectra of Cu_n ($n = 2$–20) clusters

Kopinjol Baishya,[1] Juan C. Idrobo,[1,2] Serdar Öğüt,[1] Mingli Yang,[3] Koblar A. Jackson,[4] and Julius Jellinek[5]

[1]*Department of Physics, University of Illinois at Chicago, Chicago, Illinois 60607, USA*

[2]*Department of Physics and Astronomy, Vanderbilt University, Nashville, Tennessee 37235, USA*

[3]*Institute of Atomic and Molecular Physics, Sichuan University, Chengdu 610065, China*

[4]*Department of Physics, Central Michigan University, Mount Pleasant, Michigan 48859, USA*

[5]*Chemical Sciences and Engineering Division, Argonne National Laboratory, Argonne, Illinois 60439, USA*

(Received 25 March 2011; published 17 June 2011)

Optical absorption spectra for the computed ground state structures of copper clusters (Cu_n, $n = 2$–20) are investigated from first principles using time-dependent density functional theory in the adiabatic local density approximation (TDLDA). The results are compared with available experimental data, existing calculations, and with results from our previous computations on silver and gold clusters. The main effects of *d* electrons on the absorption spectra, quenching the oscillator strengths, and getting directly involved in low-energy excitations increase in going from Ag_n to Au_n to Cu_n due to the increase in the hybridization of the occupied, yet shallow, *d* orbitals and the partially occupied *s* orbitals. We predict that while Cu nanoparticles of spherical or moderately ellipsoidal shape do not exhibit Mie (surface plasmon) resonances, unlike the case for Ag and Au, extremely prolate or oblate Cu nanoparticles with eccentricities near unity should give rise to Mie resonances in the lower end of the visible range and in the infrared. This tunable resonance predicted by the classical Mie-Gans theory is reproduced with remarkable accuracy by our TDLDA computations on hypothetical Cu clusters in the form of zigzag chains with as few as 6 to 20 atoms.

DOI: 10.1103/PhysRevB.83.245402 PACS number(s): 78.67.−n, 36.40.Vz, 73.22.−f, 61.46.Bc

I. INTRODUCTION

Clusters form a bridge between the atomic and the condensed phases of matter. Due to quantum effects and their large surface to volume ratios, their properties are typically quite different from those of the bulk. Studies of the evolution of cluster properties as a function of size can help in understanding the origin of bulk properties as well as in tailoring their size and geometric arrangements to bring out novel effects at the nanoscale. Over the past two decades, such studies have been the focus of intense research due to their fundamental importance and potential technological applications. Some of the main factors that influence the properties of clusters are size, geometric packing (atomic structure), and the electronic structure of the constituent elements. These factors ultimately determine the overall characteristics and the response of clusters to external fields, such as static polarizabilities, photoelectron spectra, or optical absorption spectra, to name a few.

Atomic, electronic, and optical properties of clusters of group IB (noble metal) elements (Ag, Au, Cu) have recently been of particular interest due to their interesting electronic structures and their promising applications in catalysis, optoelectronics, and nanophotonics. At the atomic level, these elements have filled, localized *d* orbitals and half-filled, delocalized *s* orbitals. While some of the characteristics of group IB clusters are, to a certain extent, similar to those of group IA clusters, as determined by their *s* valence electrons, the close proximity of the *d* orbitals in the atom and the corresponding *d* band in bulk materials significantly modifies their structural, electronic, and optical properties. Among them, Cu clusters are particularly challenging from a computational point of view since the relevant atomic 3*d* wave functions are nodeless, making these valence orbitals highly localized. In addition, among coinage elements, the *s*-*d* energetic separation is the smallest for Cu; as such, the *d* electrons significantly affect various properties of Cu clusters due to their strong hybridization with *sp* electrons.

There have been several experimental studies on the structural, electronic, and optical properties of Cu_n clusters.[1–17] More than three decades ago, Moskovits and Hulse[1] reported their absorption spectra in the size range from $n = 1$–4 obtained in CH_4 and Ar matrices. Cu_2 has been investigated in detail by several groups; the results from earlier studies[2–6] were summarized by Morse.[7] More recently, photoelectron spectroscopy,[11–14] chemical reactivity,[15] ionization potential,[16] and electric dipole polariability[17] studies of Cu_n have been reported by various groups. Theoretically, there have been many investigations on the structural and electronic properties of Cu_n clusters.[18–39] Optical properties have been investigated to a lesser degree. Following the work of Moskovits and Hulse, Anderson[40] interpreted their experimental data using a molecular orbital theory with superimposed rigid atom Fock potentials. Witko and Beckmann used the multireference double excitation configuration method to calculate the excited state properties of the Cu_2 molecule.[41] More recently, Wang *et al.* performed a detailed study of Cu_2 within the time-dependent density functional theory (TDDFT) using the hybrid Becke three-parameter Lee-Yang-Parr (B3LYP) functional.[42] Optical properties of free and MgO(100)-supported Cu_n clusters have been investigated by Del Vitto *et al.*[43] for $n = 1,2,4$ using B3LYP-TDDFT and complete active space second-order perturbation theory (CASPT2); by Bosko *et al.*[44] for $n = 1$–2; and by Huix-Rotllant *et al.*[45] for $n = 2$ using TDDFT with the Becke and Perdew (BP86) functional. Recently, Zhou and Zeng performed a TDDFT study of Cu_n ($n = 3$–9) clusters using the Amsterdam density functional code.[46] Most recently, Lecoultre *et al.*[47] presented a joint experimental/theoretical

(B3LYP-TDDFT) study of the optical properties of Cu_n ($n = 1$–9) clusters.

During the last several years, our group has been performing first-principles studies on various properties of small to medium size noble metal clusters, Ag_n and Au_n, with an emphasis on their optical properties using TDDFT and GW-Bethe-Salpeter-equation methods.[48–53] In this paper we continue to present results from and analyses on our first-principles investigations of noble metal clusters, focusing on a systematic study of the optical properties of Cu_n clusters in the $n = 2$–20 size range using TDDFT within the adiabatic local density approximation (TDLDA). We perform comparisons of our theoretical spectra with available experimental data and obtain generally reasonable agreement. We also compare our results with those from previous computations for Cu_n for the available sizes, as well as with our previous TDLDA results for Ag_n and Au_n clusters. We show that the two main effects of d electrons related to the quenching of the oscillator strengths and getting involved in low-energy excitations are significantly enhanced in going from Ag_n to Au_n to Cu_n due to the stronger s-(p)-d hybridization. Finally, we show that while the absorption spectra of spherical or moderately ellipsoidal Cu clusters do not exhibit Mie resonances,[54,55] unlike the case for Ag_n and Au_n (Refs. 52 and 56), extremely oblate or prolate Cu_n clusters are predicted to have large and tunable absorption cross sections in the visible and infrared (IR) regions of the spectrum. We further show that this prediction from a classical theory is reproduced remarkably well via TDLDA calculations on various highly prolate hypothetical Cu_n clusters. The rest of the paper is organized as follows. In the next section, we outline the theoretical background of the details of the computational methodologies used in this study. The results and the discussion of the optical spectra in terms of comparisons with the experiment and other computations, the effects of the d electrons, comparison with Ag_n and Au_n clusters, and predictions from Mie-Gans theory are presented in Sec. III. We conclude with a brief summary in Sec. IV.

II. THEORETICAL BACKGROUND AND COMPUTATIONAL METHODS

The Cu_n ($n = 2$–20) clusters considered in this study are the ground state structures obtained for each size in Refs. 35 and 36, as shown in Fig. 1. For each size larger than $n = 7$, the structure was obtained from an extensive search for the minimum energy geometry. The search strategy made use of an unbiased scheme for generating a large number of randomly arranged structures, and a fast, but approximate tight-binding method to relax each structure to a local minimum on the tight-binding energy surface. From this large pool, up to 500 of the lowest-energy structures at each cluster size were selected for further study. The energetic ordering of these structures was then refined by doing a single, fully self-consistent density functional theory (DFT) calculation at the corresponding tight-binding geometries. Finally, based on these single-point DFT energies, up to 30 of the lowest-energy structures were selected for full relaxation within DFT. Geometry optimizations were carried out within the framework of DFT using the NRLMOL code. For the DFT calculations we used generalized gradient approximation (GGA) with the Perdew-Burke-Ernzehoff

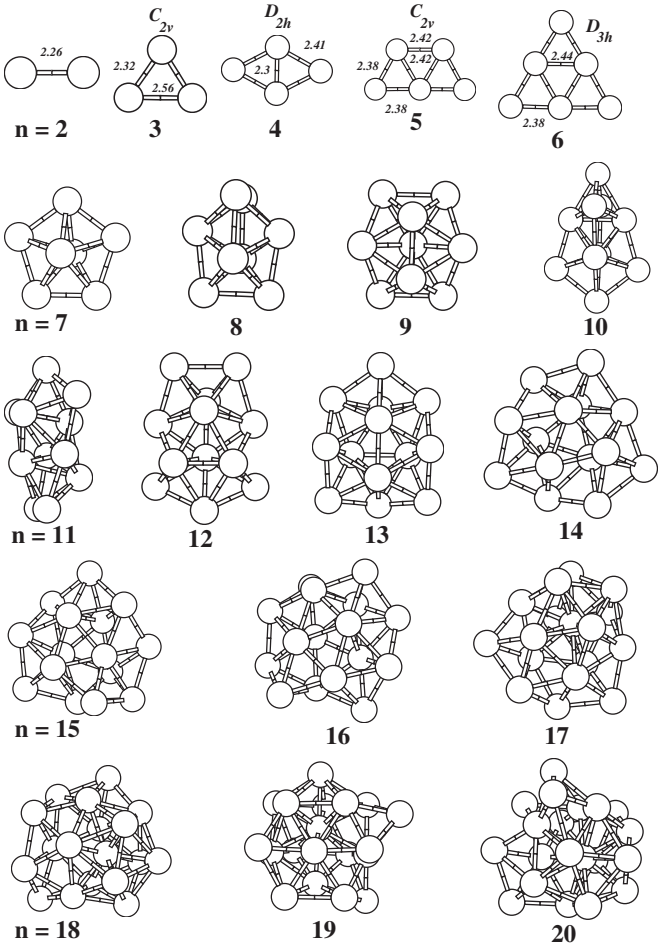

FIG. 1. Calculated ground state geometries of Cu_n ($n = 2$–20) clusters. Bond lengths (in Å) and the symmetries are displayed for clusters up to $n = 6$.

(PBE) approximation and an extensive all-electron basis set of 20 bare Gaussians contracted to $[7s5p4d]$ of each atom. The lowest-energy structure among these was then taken to be the ground state structure.

Our calculations for the absorption spectra were performed within the framework of TDLDA. We followed the frequency domain formalism of Casida, in which the excitation energies Ω_n and the corresponding oscillator strengths f_n are the poles and residues, respectively, of the dynamical polarizability $\alpha(\omega) = \sum_n f_n/(\Omega_n^2 - \omega^2)$. These two quantities are calculated by diagonalizing the full TDLDA matrix that includes all collective excitations. The entries of this matrix are computed using the wave functions and eigenvalues corresponding to the occupied and unoccupied single-particle Kohn-Sham (KS) states. The total number of unoccupied states included in the computation of the TDLDA matrix was enough to ensure convergence of absorption spectra up to ~ 6 eV in energy. The resulting matrix sizes ranged from 5000 (Cu atom) to 18 000 (Cu_{20}). Since Cu_n clusters with an odd number of atoms have an odd number of valence electrons, they call for a spin-polarized treatment, which significantly increases the time needed to set up the TDLDA matrix and diagonalize it. Even though the difference between spin-polarized and spin-unpolarized TDLDA computations are not too significant,

we performed all TDLDA computations for clusters with an odd number of atoms using explicit spin polarization.

The computations for the ground state KS eigenpairs were carried out in real space within the framework of the higher-order-finite-difference *ab initio* pseudopotential method using the PARSEC code.[57] We use scalar-relativistic Troullier-Martins pseudopotentials in nonlocal form generated from the $3d^{10}4s^{1}4p^{0}$ reference configuration with the same core radius of 2.25 a.u. for all angular momentum channels. Our tests showed that the nodeless nature of the $3d$ all-electron wave function requires a rather small grid spacing of $h = 0.3$ a.u. for the convergence of optical absorption spectra. This is a more stringent choice than the cases for Ag or Au, for which $h = 0.4$ or 0.5 a.u. are adequate for achieving similar convergence. The clusters were placed inside a spherical domain of radius $R_{\max} = 24$ a.u. outside of which the wave functions were required to vanish. With the above choices of $R_{\max}$ and h, the resulting dimension of the KS Hamiltonian is $\sim 2 \times 10^6$. For diagonalization and iteration to self-consistency, we used a Chebysev-Davidson eigenvalue algorithm that uses subspace filtering with Chebysev polynomials once an initial set of KS eigenpairs is known.[58]

III. RESULTS AND DISCUSSION

A. Structures

Figure 1 shows the computed ground state structures of Cu_n clusters, which display an interesting evolution of geometrical features. The smaller clusters, up to $n = 6$, are planar with a trigonal bonding motif. From $n = 8$ to 16, the clusters adopt a layered structure, with no interior atoms. From $n = 9$ to 11 they are prolate. Cu_{12} and Cu_{13} are triaxial. Larger clusters are oblate, but become more compact and spherical toward $n = 20$. From $n = 17$ to 20, they are able to accommodate an interior atom. As discussed elsewhere, the evolution of cluster shape from $n = 8$ to 20 can be explained in terms of shell fillings and the jellium model.[36]

B. Optical absorption spectra

The optical absorption spectra of Cu_n, $n = 2$–20, are plotted in Figs. 2 and 3. For the Cu atom, we compute the $4s \rightarrow 4p$ transition energy at 4.19 eV with an oscillator strength (OS) of $f = 0.32$. Compared to Ag with a computed OS of 0.63 for the $5s \rightarrow 5p$ transition, the large reduction in f is due to the increased screening of the s electrons by the d electrons. The experimental spin-orbit averaged value for this transition is 3.81 eV (Ref. 59). The TDLDA overestimates the $s \rightarrow p$ transition energy by $\sim$10%, similar to those observed for Ag and Au. Our values are in reasonable agreement with the computed values reported by Del Vitto *et al.*[43] who found $4s \rightarrow 4p$ transition energies of 3.89 eV (B3LYP-TDDFT) and 4.03 eV (CASTP2) with an OS of $f = 0.27$ for the latter, and by Bosko *et al.*[44] who found a transition energy of 4.12 eV with $f = 0.15$. We find the next strong TDLDA transition at 5.17 eV with $f = 0.38$. This corresponds to the $3d \rightarrow 4p$ transition experimentally measured at the spin-orbit averaged value of 5.47 eV. Our computed values for the optically forbidden

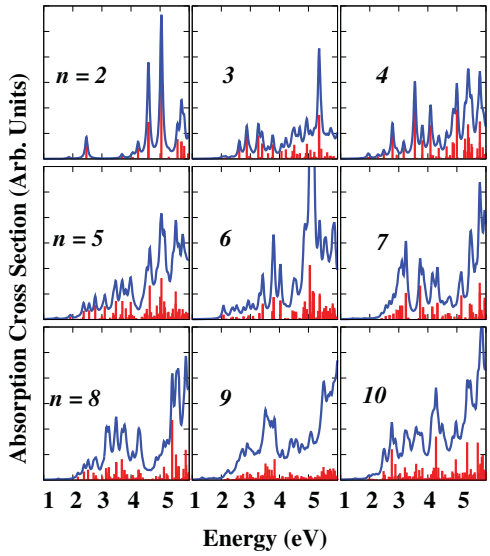

FIG. 2. (Color online) TDLDA spectra of Cu_n clusters for sizes $n = 2$–10. The spectra were broadened using Lorentzians of half-width 0.1 eV.

$3d \rightarrow 4s$ and $4s \rightarrow 5s$ transitions are 0.90 and 5.22 eV, which compare reasonably well with the values of 1.10 and 5.18 eV obtained by Bosko *et al.*, and experimentally measured at 1.49 and 5.35 eV, respectively. The comparisons of our TDLDA results for the Cu atom with other TDDFT computations and experiments are summarized in Table I.

For Cu_2 our computed TDLDA transitions with nonvanishing OS below $\sim$5 eV are at 1.86 ($f = 0.005$), 2.47 ($f = 0.067$), 3.69 ($f = 0.012$), 4.06 ($f = 0.013$), 4.24 ($f = 0.044$), 4.60 ($f = 0.29$), and 5.04 eV ($f = 0.44$). We assign

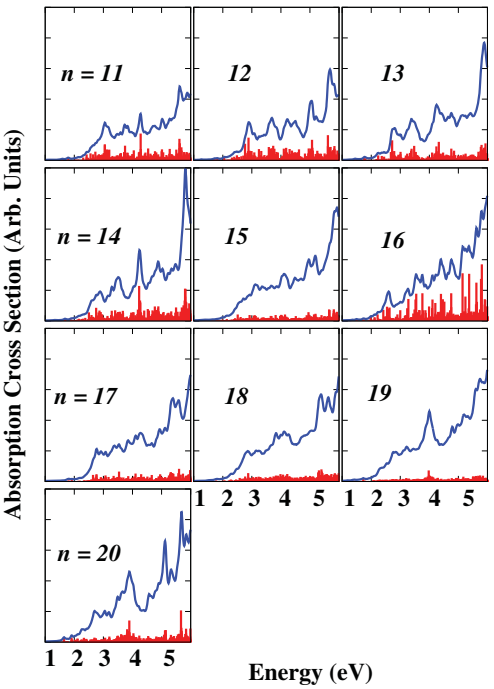

FIG. 3. (Color online) TDLDA spectra of Cu_n clusters for sizes $n = 11$–20. The spectra were broadened using Lorentzians of half-width 0.1 eV.

TABLE I. Comparison of experimental absorption energies, our computed TDLDA values (in eV) and oscillator strengths (OS) and results from other TDDFT treatments for Cu and Cu_2. Values in parentheses next to the excitation energies are the corresponding OS. The experimental data for Cu_2 are taken from Refs. 7 and 47. For the Cu atom, they are taken from Ref. 59.

		Computed Excitation Energy (OS)				
Transition	Experiment	This work	Wang *et al.* (Ref. 31)	Lecoultre *et al.* (Ref. 47)	Del Vitto *et al.* (Ref. 43)	Bosko *et al.* (Ref. 44)
Cu						
$4s \rightarrow 4p$	3.81	4.19 (0.32)	–	6.00	3.89	4.12 (0.15)
$3d \rightarrow 4p$	5.47	5.17 (0.38)	–	6.30	–	–
$3d \rightarrow 4s$	1.49	0.90 (0.00)	–	–	1.38 (0.00)	1.10 (0.00)
$4s \rightarrow 5s$	5.35	5.22 (0.00)	–	–	–	5.18 (0.00)
Cu_2						
$X \rightarrow a$	1.91	1.86	1.93	–	–	1.91
$X \rightarrow A$	2.53	1.99	2.60	2.62	–	–
$X \rightarrow B$	2.70	2.47	2.86	2.85	2.89	2.53
$X \rightarrow C$	2.71	2.67	3.00	–	–	–
$X \rightarrow D$	3.17	3.69	3.66	–	–	3.67
$X \rightarrow J$	4.64	4.60	4.72	–	–	–
Ref. 47	4.10	(4.06–4.24)	–	–	–	–
Ref. 47	5.08	5.04	–	–	–	–
Ref. 47	5.41	(5.55–5.73)	–	–	–	–

our computed transition at 1.86 eV to the $X \rightarrow a$ transition experimentally measured at 1.91 eV. From intensity considerations, our computed transition at 2.47 eV is assigned to the $X \rightarrow B$ transition measured experimentally at 2.70 eV, not the $X \rightarrow A$ transition measured at 2.53 eV which has a much smaller OS, and which we accordingly associate with our computed transition at 1.99 eV with an almost vanishing OS. Similar to the assignment of Wang *et al.*, the $X \rightarrow C$ transition measured at 2.71 eV with its very weak oscillator strength is associated with our computed dark transition at 2.67 eV. Our computed transition at 3.69 eV is assigned to the $X \rightarrow D$ transition measured at 3.17 eV. The TDLDA transition at 4.60 eV with a large OS of $f = 0.29$ is assigned to the strong $X \rightarrow J$ transition measured at 4.64 eV. For the rest of the measured transitions reported in Ref. 7, the particular assignments to our computed TDLDA transitions are more difficult and would be somewhat speculative. It is important to note, however, that our TDLDA results compare reasonably well with the most recent experimental data by Lecoultre *et al.*[47] In particular, at energies above 4 eV, the agreement is very good. The high intensity absorption peaks measured by Lecoultre *et al.* at 4.10, 4.68 ($X \rightarrow J$), 5.08, and 5.41 eV are assigned to our computed transitions at (4.06–4.24), 4.60, 5.04, and (5.55–5.73) eV, respectively, where the values in parentheses denote the range within which a few computed peaks could correspond to the observed line. At lower energies, the agreement with the new experiments is not as good. Interestingly, the exact opposite trend is observed in the comparison of TDDFT computations of Lecoultre *et al.* with their experimental data. At low (2–3 eV) energies (for $X \rightarrow A$ and $X \rightarrow B$ transitions), their computations agree quite well with their experiments, while the agreement is not good at higher energies. The effect of different exchange-correlation functionals used in the two computations is the most likely reason for the discrepancies between the two sets of computations. The comparisons of our TDLDA results for Cu_2 with other TDDFT computations and experimental data in Refs. 7 and 47 are summarized in Table I.

The TDLDA spectrum for Cu_3 starts with a series of small peaks in the 2.0–2.40 eV energy range followed by significant peaks at 2.62 ($f = 0.05$), 2.88 ($f = 0.09$), 3.27 ($f = 0.09$), 3.41 ($f = 0.06$), 3.77 ($f = 0.065$), 4.51 ($f = 0.06$), 4.94 ($f = 0.06$), and 5.36 eV ($f = 0.31$). These values agree fairly well with the measured peak positions, but not quite with the measured intensities, in the most recent experiments of Lecoultre *et al.* that found main absorption lines at 2.66, 2.91, 3.37, 3.49, 3.70, 4.45, (4.78–4.94), and (5.17–5.30) eV. However, the sharp experimental peak measured at 2.46 eV is not accounted for in our TDLDA computations, unless one assigns it to some of the very-low intensity peaks computed between 2.30 and 2.40 eV in the TDLDA computations. The sampling of a different isomer and matrix effects in the experiments, inaccuracy associated with the level of theory, or a combination of these might be the more likely reasons for this discrepancy. In fact, the recent TDDFT computations of Lecoultre *et al.* did not find any sharp peak near 2.5 eV for the ground state cluster of C_{2v} symmetry either. Instead, they suggested that the experimental peak at 2.46 eV is in better agreement with a high-intensity peak they computed at 2.67 eV for the linear ($D_{\infty h}$) Cu_3 cluster. Indeed, our computation for the linear trimer does find a transition with a large oscillator strength of $f = 0.19$ at an energy of 2.71 eV that could possibly correspond to the sharp experimental peak at 2.46 eV. Our orbital decomposition analysis for the ground state (C_{2v}) structure of Cu_3 shows that the lower-energy peaks have considerable weight from transitions that originate from highest-occupied molecular orbital (HOMO) (in the spin-up channel), which is a largely (80%) sp hybrid, while the rest of the weight is attributed to transitions from the d-like orbitals to lowest-unoccupied molecular orbital (LUMO) (in the spin-down channel). Above 3 eV, the weight attributed to transitions from HOMO goes down considerably, and the transitions are

mostly from d-like states to low-lying unoccupied orbitals of largely p character with some s admixture.

The TDLDA spectrum for Cu_4 exhibits five major peaks below 5.5 eV, located at 2.78 ($f = 0.104$), 3.55 ($f = 0.227$), 4.09 ($f = 0.132$), 5.00 ($f = 0.193$), and 5.38 eV ($f = 0.136$). In addition, there are secondary peaks of lesser intensity near 1.95 eV (onset of absorption), 2.48, 3.17, 3.81, 4.37, 4.64, and 4.87 eV. The agreement with results from the most recent experiments of Lecoultre *et al.* is good for the tetramer: In particular, the large peaks at 2.93, 3.54, and 4.90 eV in the experiments are reproduced well in our computations. In agreement with the interpretation of Moskovits and Hulse, the low-energy transition computed at 2.92 eV is associated with transitions from predominantly $3d$ character to LUMO + 1, which is an sp hybrid with large $4s$ character. We note that our results also seem to be in very good agreement with the results of Del Vitto *et al.* who found (i) the first TDDFT transition at 1.19 eV with zero OS (our first zero-OS transition is at 1.16 eV), and (ii) a significant peak at 2.80 eV with $f = 0.102$ to be compared with ours at 2.78 eV ($f = 0.104$). Our computations also have somewhat good agreement with the most recent computations of Lecoultre *et al.*

For the rest of the clusters, the data are presented in Figs. 2 and 3. Overall, compared with the most recent experimental results of Lecoultre *et al.*[47] there is reasonable agreement (especially for $n = 7$–9, but not so much for $n = 5$–6), although there are differences in some cases, which mostly can be attributed to the combination of (i) the limitations of TDLDA, (ii) the likely possibility of more than one isomer contributing to the experimental spectrum,[60] and (iii) the effects of the solid neon matrix in which the clusters were embedded in the experiments on the positions of the spectral lines and their intensities. Our computations displayed in Figs. 2 and 3 show that as the cluster size gets larger, the corresponding spectra evolve into more continuous distributions of peaks with low OS. The spectra for larger sizes typically start with an absorption onset near 2 eV, and display a shoulder near 2.5 eV and a local maximum near 4 eV, all of which can be correlated with the features observed in the imaginary part $\epsilon_2(\omega)$ of the dielectric function of bulk Cu. Further discussion on this is given in the next section when the spectra are discussed in the classical Mie theory framework.

C. Comparison with Ag and Au

1. Integrated oscillator strengths

In our previous studies for Ag_n and Au_n clusters, we showed that the screening of the s electrons due to d electrons (core polarization effects) in noble metal clusters results in the quenching of the oscillator strengths and a redshift of the plasmon frequency. Clusters of Cu, which has the smallest s-d energy separation at the atom level among the three group IB elements, are expected to show a higher core polarization effect. Figure 4 shows the calculated size dependence of the oscillator strengths integrated up to a cutoff energy of 6 eV for Cu_n clusters, along with the same values for Ag_n and Au_n clusters. On average, the quenching is highest in Cu_n clusters. Above $n \sim 8$, the integrated oscillator strengths (IOS) of Cu_n are significantly lower (by a factor of ~2) than those of

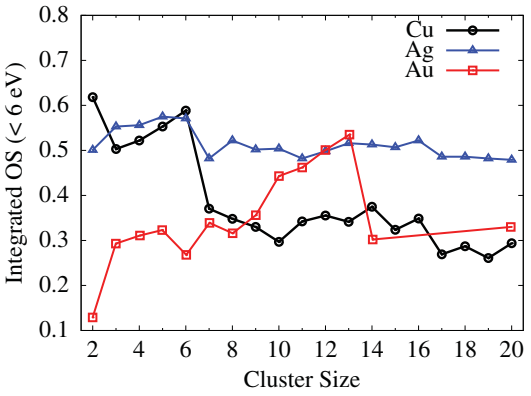

FIG. 4. (Color online) The oscillator strengths per s electron of the Cu_n clusters (black lines with circles) integrated up to $E_c = 6$ eV as a function of the cluster size. Also shown are the same results for Ag_n (blue lines with triangles) and Au_n (red lines with squares) clusters.

Ag_n. The deviation from this trend observed at smaller sizes is due to the fact that the discrete d-like excitations in Ag_n typically occur at much higher energies above 6 eV, while for Cu_n clusters the IOS below 6 eV have a large contribution from sharp excitations originating from orbitals of d character and much less from orbitals of sp character. As discussed in detail in Ref. 51 for the case of Au_n clusters, the overall size dependence of IOS for Cu_n clusters is very similar to the size dependence of their static polarizabilities.[36] The significant drops in IOS at $n = 7$ for clusters of Ag and Cu, and at $n = 14$ for clusters of Au are correspondingly associated with the transition from from two-dimensional to more compact three-dimensional structures.

2. Orbital character of TDLDA excitations

In addition to quenching the oscillator strengths, another way in which the d electrons affect the optical spectra of noble metal clusters is getting directly involved in low-energy excitations. Similar to the case of quenched oscillator strengths, the degree to which the d electrons become involved in low-energy excitations is largest in Cu_n clusters. This can already be inferred by the rather small energy separation of the $3d$-$4s$ atomic levels, which results in a large s-(p)-d hybridization in the molecular orbitals of Cu_n clusters.

A comparison of the orbital characters of the occupied and low-lying unoccupied molecular orbitals for Ag_2 and Cu_2 clusters is instructive in understanding the differences between the orbital characters of the low-energy optical excitations computed for the two noble metal dimers. In Ag_2, due to the large $4d$-$5s$ atomic separation, the d orbitals hybridize among themselves, practically decoupled from the s orbitals, which makes the first ten doubly occupied KS levels (counting spin, but not orbital degeneracies) have almost purely d character, while the HOMO and the LUMO are bonding and antibonding combinations of $5s$ orbitals. In Cu_2, the large hybridization results in KS orbitals of mixed s-d character with even some p admixture. As shown in Fig. 5, there is no direct analog of a bonding combination of $4s$ levels at the local density approximation (LDA) level for any of the occupied KS levels of Cu_2. HOMO (doubly degenerate), HOMO-1, HOMO-2

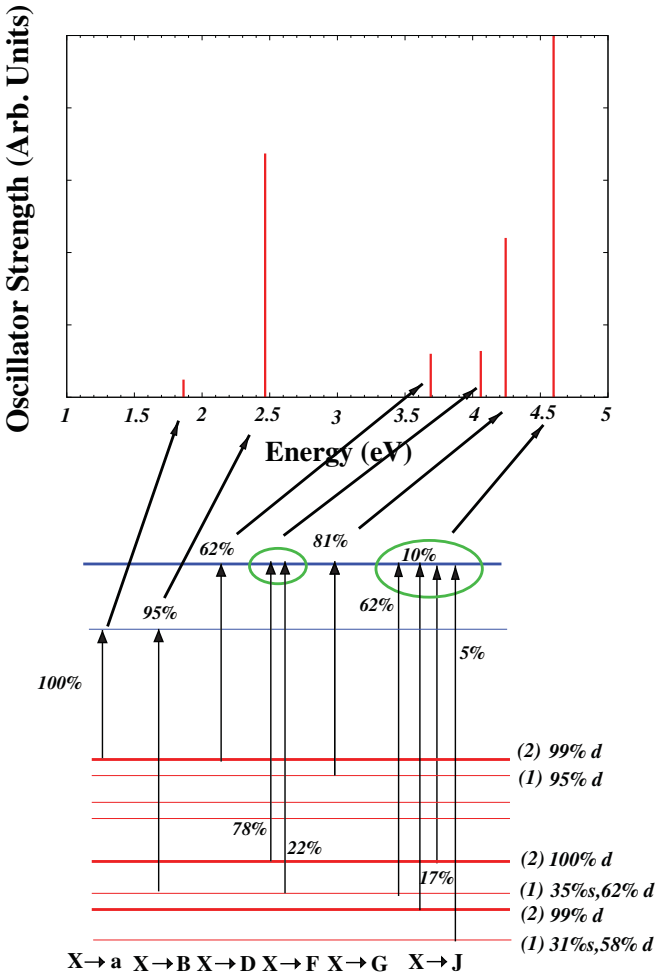

FIG. 5. (Color online) The Kohn-Sham energy levels (within LDA) of Cu_2 that are involved in the excitations at 1.86 ($X \rightarrow a$), 2.47 ($X \rightarrow B$), 3.69 ($X \rightarrow D$), 4.06, 4.24, and 4.60 ($X \rightarrow J$) eV. The degeneracies (in parentheses) and the angular characters of the occupied (shown in red) and unoccupied (shown in blue) orbitals involved in the transitions are given next to the energy levels. The weights (in %) of the vc orbital pairs in the eigenvectors of the transitions are also shown. See the text for details.

(doubly degenerate), and HOMO-3 (doubly degenerate) all have d character with negligible or no sp contribution. The levels with the largest sp character are HOMO-4 and HOMO-6 (the first occupied molecular orbital). Even for these levels, the combined sp characters are only 38% and 42%, respectively. For Au_2, which can be considered intermediate in terms of s-d hybridization between Ag_2 and Cu_2, the KS level with the largest s character appears as HOMO-2 with a considerable 85% s character.[51]

This large hybridization observed in the KS levels of Cu_2 naturally affects the orbital characters of the optical transitions. Using the same analysis as described in Refs. 48 and 51, we have investigated the orbital characters of some of the low-energy TDLDA transitions in Cu_2 by identifying the few dominant occupied-unoccupied (or valence-conduction, vc) pairs that appear in the TDLDA eigenvector for a given transition. As shown in Fig. 5, the first transition observed at 1.86 eV, assigned to the experimental $X \rightarrow a$ line, involves entirely the HOMO/LUMO vc pair. Given that HOMO in Cu_2 is of purely d character, we immediately observe that the lowest allowed optical transition in Cu_2 has entirely d character. In Ag_2, even though the first allowed optical transition computed near 3.2 eV also involves primarily the HOMO/LUMO vc pair (95% in its TDLDA decomposition) since HOMO in Ag_2 almost entirely has s character, the associated optical transition involves s electrons. As mentioned above, since Cu_2 has no direct analog of a KS level with entirely s character (i.e., the analog of HOMO in Ag_2), there is no obvious optical transition associated with s electrons. The transition that comes close to being most s like is the one computed at 2.47 eV, assigned to the $X \rightarrow B$ line, that is a 95% mixture of HOMO-4/LUMO and 5% of HOMO-6/LUMO vc pairs with the largest sp characters among the occupied KS levels. It is interesting to observe that this "most s like" transition pairing HOMO, HOMO-2, and (HOMO-4,HOMO-6) occupied states with LUMO for Ag_2, Au_2, and Cu_2 occurs at energies of 3.16, 2.71, and 2.47 eV, respectively. The gradual redshift in the energy of this most s like optical transition is an indication of the enhanced core-polarization effect in going from Ag to Au to Cu. Some of the other low-energy optical transitions with their dominant vc pairs are shown in Fig. 5. The analysis shows that the transitions computed at 4.06 and 4.24 eV, for example, are primarily $3d$ to $4p$ transitions as they involve, to a large extent, LUMO + 1 and LUMO + 2 which are almost entirely p-like orbitals, while the dominant occupied orbitals involved in both are those with entirely d character. Finally, it is interesting to note that the transition computed at 4.60 eV is mostly associated with the HOMO-4/LUMO + 1 vc pair, which indicates that this is the closest analog of the $5s$ (HOMO) to $5p$ (LUMO + 1) transition computed at the higher energy of 4.75 eV in Ag_2, in accordance with the decreased core polarization in the latter.

To further quantify the various orbital contributions to the optical spectra, we computed the percentages of the s, p, and d characters in the transitions following the same method, as described in Refs. 48 and 51. For example, the percent of the integrated d electron contributions over a range with a cutoff value of E_c is defined as

$$\%d = \frac{\sum\limits_{i,\Omega_i<E_c} f_i \sum\limits_{vc} \left|F_i^{vc}\right|^2 |\langle d|\phi_v\rangle|^2}{\sum\limits_{i,\Omega_i<E_c} f_i} \times 100, \qquad (1)$$

where $\langle d|\phi_v\rangle$ is the projection of the occupied KS orbital $\phi_v(\mathbf{r})$ to the d atomic wave function (summed over all magnetic quantum numbers), and F_i^{vc} are the entries, labeled by vc pairs, of the TDLDA eigenvector corresponding to a particular transition with oscillator strength f_i and excitation energy of Ω_i. A plot of the d character up to the cutoff energy of $E_c = 6$ eV as a function of cluster size for Cu_n clusters is shown in Fig. 6, along with our results for Ag_n and Au_n clusters at available sizes. As is readily evident, the integrated d contributions to the optical spectra even for small Cu_n clusters are already rather large, in contrast to those for Ag_n and Au_n (e.g., the contribution is 76%, 37%, and 16% for Cu_2, Au_2, and Ag_2, respectively). Overall, at almost all sizes the integrated d contribution increases in going from Ag_n to Au_n to Cu_n, as

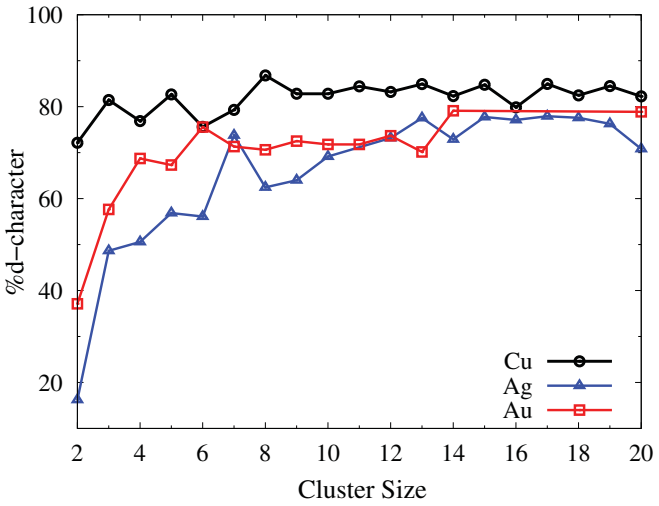

FIG. 6. (Color online) The percentage of the d character in the transitions calculated according to Eq. (1) for Cu_n (black lines with circles) as a function of n at a cutoff energy of $E_c = 6$ eV. Also shown are the same results for Ag_n (blue lines with triangles) and Au_n (red lines with squares).

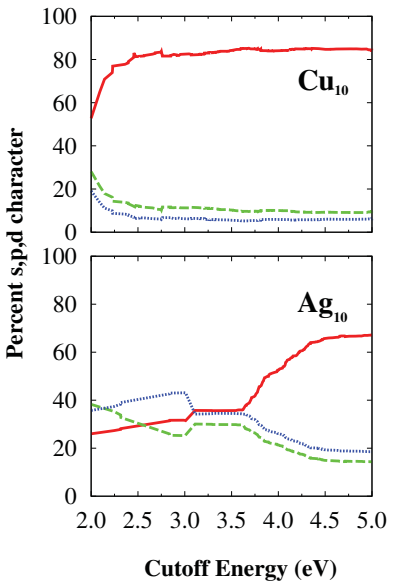

FIG. 7. (Color online) The percentages of the s (blue dotted lines), p (green dashed lines), and d (red solid lines) characters in the optical transitions for the ground state structures of Cu_{10} (upper panel) and Ag_{10} (lower panel).

expected from the trend in the degree of the proximity of the atomic d level to the s level.

For a closer look at how the the various orbital contributions change with the cutoff energy E_c, we computed s, p, and d characters of the transitions for Cu_n clusters. Figure 7 shows the s, p, and d contributions for Cu_{10} as a function of E_c, in comparison to the case for Ag_{10}, which has the same structure as Cu_{10}. One can immediately notice that not only are the integrated d contributions much larger for Cu_{10} at any energy E_c, but the sharp rise in the d character of the optical transitions occurs at much lower energies (∼2 eV) for Cu_{10} compared to Ag_{10} (above ∼3.6 eV), indicating the degree with which the d electrons are involved in very low-energy optical excitations of Cu_n clusters.

3. *TDLDA versus predictions from Mie-Gans theory*

In recent studies, we showed that the optical spectra of Si_n ($n = 20$–28 in Ref. 61) and Ag_n ($n = 10$–20 in Ref. 52) clusters computed with TDLDA could be reproduced remarkably well by the classical Mie-Gans theory using the corresponding bulk dielectric functions. For an ellipsoidal object in a vacuum with semi-axes A, B, and C, the Mie-Gans theory gives the following expression for the absorption cross section:

$$\sigma_{\rm abs}(\omega) = \frac{4\pi\omega ABC}{9c} \times \sum_{i=1}^{3} \frac{\epsilon_2(\omega)}{[1 + G_i(\epsilon_1(\omega) - 1)]^2 + [G_i\epsilon_2(\omega)]^2}. \quad (2)$$

In this expression, $\epsilon_1(\omega)$ and $\epsilon_2(\omega)$ are the real and imaginary parts of the bulk dielectric function, c is the speed of light, and the depolarization factors G_i, which satisfy $\sum_{i=1}^{3} G_i = 1$, are related to the shape of the ellipsoid.[62] While spherical Si, Ag, and Au nanoparticles ($G_1 = G_2 = G_3 = 1/3$) exhibit Mie (surface plasmon) resonances near 9.8, 3.5, and 2.5 eV, respectively, such a feature does not exist in spherical Cu nanoparticles. The Mie resonance for spherical particles in a vacuum occurs when $\epsilon_1(\omega) = -2$ if $\epsilon_2(\omega)$ is relatively small. This condition is not satisfied with the bulk dielectric function of Cu. The physical reason for this is the close proximity of the d band to the s band in bulk Cu. The positive *interband* contribution to $\epsilon_1(\omega)$ of Cu occurs at a much lower threshold energy (near 2 eV) where the Drude contribution $(1 - \omega_p^2/\omega^2)$ to $\epsilon_1(\omega)$ from the *intraband* transitions are much too negative[63] to produce an almost zero crossing necessary for a plasmon resonance. As a result, the Mie absorption spectrum of a spherical nanoparticle has no sharp resonance: It starts smoothly near 2 eV, has small shoulder-like bumps near 2.5 and 4 eV (corresponding to transitions up from the conduction band,[64]) and rises continuously. The TDLDA spectrum for the ground state structure of Cu_{20}, which is the most spherical cluster in this size regime as determined by the computed normalized moments of inertia,[52] is shown in Fig. 8(a) along with the predictions from the Mie theory of a spherical Cu nanoparticle. Even though the absence of a sharp resonance in the spectra (unlike the case of Ag or Au) makes the validity of a good agreement between the TDLDA and Mie predictions hard to argue in a compelling fashion, the onset near 2 eV and the features near 2.5 and 4 eV resemble each other somewhat well.

While the Mie-Gans spectra of spherical or moderately prolate/oblate Cu clusters do not exhibit sharp resonances, we observed that more interesting scenarios for Cu occur, if one concentrates on extremely prolate or oblate clusters with eccentricities $e \sim 1$. For example, for prolate clusters with $G_1 = G_2 \gtrsim 0.45, G_3 \lesssim 0.1$, Mie-Gans theory predicts a large resonance at the lower end of the visible spectrum or in the IR. The position of the large resonance is tunable by changing the eccentricity of the clusters; it shifts to lower energies and grows in intensity as the cluster becomes more and more prolate as

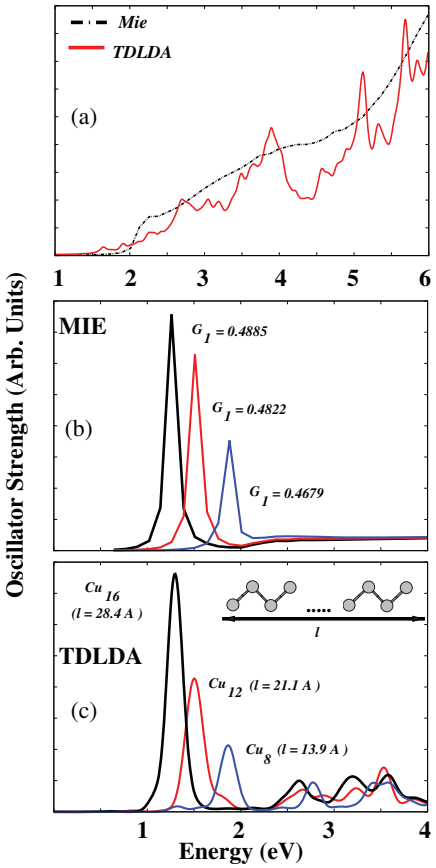

FIG. 8. (Color online) (a) TDLDA spectrum for the ground state structure of Cu_{20} in comparison with the Mie-theory prediction for a spherical particle using the bulk dielectric function of copper. (b) Mie-Gans prediction and (c) TDLDA results for three zigzag Cu chains of composition Cu_8, Cu_{12}, and Cu_{16}. The depolarization factors G_1 are computed from the measured dimensions of the corresponding chains as discussed in the text. $G_2 = G_1$ and $G_3 = 1 - G_1 - G_2$. See the text for more details.

shown in Fig. 8(b) for various depolarization factors that give rise to peaks between 1 and 2 eV. To find out whether such a behavior is also predicted by TDLDA, we performed computations on hypothetical extremely prolate Cu clusters in the form of long chains. We created the clusters from the zigzag chain of atoms along the [100] direction of bulk Cu. We created five chain clusters of composition Cu_6, Cu_8, Cu_{12}, Cu_{16}, and Cu_{20}. The results from TDLDA computations on these chain clusters indeed show large resonances ranging from near 2.0 eV (Cu_6) to 1.1 eV (Cu_{20}) with intensities increasing as the size of the cluster (its eccentricity) increases. The TDLDA results for Cu_8, Cu_{12}, and Cu_{16} are shown in Fig. 8(c), which shows a remarkable agreement with Mie-Gans predictions. It is important to note that the agreement between TDLDA and Mie-Gans predictions is not just qualitative, but rather accurate in terms of the peak positions as predicted from the geometrical factors. For example, measuring the semi-axes A and B of the Cu_{12} chain as 21.13 and 3.08 Å, respectively (we add half a bulk Cu bond length to the ends in each direction to mimic charge spill-out), we calculate an eccentricity of $e = 0.989\,32$ which gives depolarization factors of $G_1 = G_2 = 0.4822$ and $G_3 = 0.0356$. The Mie-Gans theory, with these G_i values and bulk Cu dielectric function, predicts a resonance at an energy of 1.51 eV, in very good agreement with the TDLDA resonance of 1.50 eV. The Mie-Gans results shown in Fig. 8(b) are indeed calculated using the exact depolarization factors as determined from the measured dimensions of the Cu_8, Cu_{12}, and Cu_{16} chain clusters. It is remarkable that the agreement between TDLDA and Mie-Gans theories holds to such a high degree of accuracy. The results presented here are also quite interesting in the sense that if such chains (or any type of extremely ellipsoidal copper nanostructures) can be synthesized as metastable clusters, they are predicted to absorb very strongly in the lower end of the visible and the IR region of the spectrum. The large absorption cross section and the tunability of the resonance energy by varying the aspect ratio of such chains (or nanowires) can be potentially important for the future design of Cu-based nanomaterials for light-harvesting applications.

IV. SUMMARY

We have continued with our systematic studies of electronic and optical properties of noble metal clusters by presenting results on and analyses of the optical absorption spectra for the computed ground state structures of Cu_n clusters ($n = 2$–20) within the framework of TDLDA. Our results are generally in reasonable agreement with existing experiments and computations for the available small sizes. We have shown that the d electrons of copper affect the optical spectra of its clusters by quenching the oscillator strengths and getting directly involved in excitations at energies as low as 2 eV. A comparison with our previous results on Ag_n and Au_n shows that among all noble metal clusters these effects are most pronounced in Cu_n clusters. Our investigations have also resulted in an interesting prediction of large Mie resonances in extremely prolate or oblate Cu nanoparticles, which are absent for the case of moderately ellipsoidal or spherical particles. These large resonances occur in the 1 to 2 eV range and are tunable by changing the eccentricity of the particles, shifting to lower energies, and growing in intensity as the nanoparticle becomes more extremely ellipsoidal. This prediction from the classical Mie-Gans theory is reproduced with remarkable accuracy by TDLDA computations on Cu clusters in the form of zigzag chains with as few as 6 to 20 atoms. If such extremely ellipsoidal Cu particles can be synthesized as (meta)stable nanomaterials, this finding could potentially be useful for light-harvesting applications.

ACKNOWLEDGMENTS

This work was supported by the US Department of Energy Grants No. DE-FG02-09ER16072 (K.B. and S.Ö.), No. FG02-09ER16061 (K.A.J.), and the Office of Basic Energy Sciences, Division of Chemical Sciences, Geosciences, and Biosciences, under Contract No. DE-AC-02-06CH11357 (J.J.). M.Y. thanks NSFC (Grant No. 20873088) and SRFDP (Grant No. 20070610175) of China. S.Ö. acknowledges support by the National Science Foundation under the Independent Research/Development program while working at the Foundation. This research used resources of NERSC, which is supported by the Office of Science of the US Department of Energy.

[1]M. Moskovits and J. E. Hulse, J. Chem. Phys. **67**, 4271 (1977).
[2]G. A. Ozin and S. A. Mitchell, J. Phys. Chem. **86**, 473 (1982).
[3]G. A. Ozin, S. A. Mitchell, D. F. McIntosh, and S. M. Mattar, J. Phys. Chem. **87**, 4651 (1983).
[4]D. E. Powers, S. G. Hansen, M. E. Geusic, D. L. Michalopoulos, and R. E. Smalley, J. Chem. Phys. **78**, 2866 (1983).
[5]M. D. Morse, J. B. Hopkins, P. R. R. Langridge-Smith, and R. E. Smalley, J. Chem. Phys. **79**, 5316 (1983).
[6]D. M. Kolb, H. H. Rotermund, W. Schrittenlacher, and W. Schroeder, J. Chem. Phys. **80**, 695 (1984).
[7]M. D. Morse, Chem. Rev. **86**, 1049 (1986).
[8]R. J. VanZee and W. Weltner, J. Chem. Phys. **92**, 6976 (1990).
[9]R. S. Ram, C. N. Jarman, and P. F. Bernath, J. Mol. Spectrosc. **156**, 468 (1992).
[10]M. B. Knickelbein, J. Chem. Phys. **100**, 4729 (1994).
[11]C. L. Pettiette, S. H. Yang, M. J. Craycraft, and J. Conceicao, J. Chem. Phys. **88**, 5377 (1988).
[12]J. Ho, K. M. Ervin, and W. C. Lineberger, J. Chem. Phys. **93**, 6987 (1990).
[13]C.-Y. Ha, G. Ganteför, and W. J. Eberhardt, J. Chem. Phys. **99**, 6308 (1993).
[14]H. Handschuh, P. S. Bechthold, G. Ganteför, and W. J. Eberhardt, J. Chem. Phys. **100**, 7093 (1994).
[15]B. J. Winter, E. K. Parks, and S. J. Riley, J. Chem. Phys. **94**, 8616 (1991).
[16]M. B. Knickelbein, Chem. Phys. Lett. **192**, 129 (1992).
[17]M. B. Knickelbein, J. Chem. Phys. **120**, 10450 (2004).
[18]J. Demuynck, M.-M. Rohmer, A. Strich, and A. Veillard, J. Chem. Phys. **75**, 3443 (1981).
[19]H. Tatewaki, E. Miyoshi, and T. Nakamura, J. Chem. Phys. **76**, 5073 (1982).
[20]G. del Conde, P. S. Bagus, and O. Novaro, Phys. Rev. A **26**, 3653 (1982).
[21]E. Miyoshi, H. Tatewaki, and T. Nakamura, J. Chem. Phys. **78**, 815 (1983).
[22]H. Åkeby and L. Pettersson, Chem. Phys. **155**, 197 (1991).
[23]D.-W. Liao and K. Balasubramanian, J. Chem. Phys. **97**, 2548 (1992).
[24]K. A. Jackson, Phys. Rev. B **47**, 9715 (1993).
[25]C. Massobrio, A. Pasquarello, and R. Car, Phys. Rev. Lett. **75**, 2104 (1995); Phys. Rev. B **54**, 8913 (1996).
[26]P. Calaminici, A. M. Köster, N. Russo, and D. R. Salahub, J. Chem. Phys. **105**, 9546 (1996).
[27]V. Musolino, A. Selloni, and R. Car, J. Chem. Phys. **108**, 5044 (1998).
[28]C. Massobrio, A. Pasquarello, and A. Dal Corso, J. Chem. Phys. **109**, 6626 (1998).
[29]M. Valiev, E. J. Bylaska, and J. H. Weare, J. Chem. Phys. **119**, 5955 (2003).
[30]M. N. Huda and A. K. Ray, Eur. Phys. J. D **22**, 217 (2003).
[31]J. Wang, G. Wang, and J. Zhao, Chem. Phys. Lett. **380**, 716 (2003).
[32]E. M. Fernandez, J. M. Soler, I. L. Garz'on, and L. C. Balbás, Phys. Rev. B **70**, 165403 (2004).
[33]W. Hong-Yan, L. Chao-Yang, T. Yong-Jian, and Z. Zheng-He, Chin. Phys. **13**, 677 (2004).
[34]H. Grönbeck and P. Broqvist, Phys. Rev. B **71**, 073408 (2005).
[35]M. Yang and K. A. Jackson, J. Chem. Phys. **122**, 184317 (2005).
[36]M. Yang, K. A. Jackson, C. Koehler, Th. Frauenheim, and J. Jellinek, J. Chem. Phys. **124**, 024308 (2006).
[37]P. Calaminici, A. M. Köster, and Z. Gómez-Sandoval, J. Chem. Theory Comput. **3**, 905 (2007); P. Calaminici, F. Janetzko, A. M. Köster, R. Meija-Olvera, and B. Zuniga-Gutierrez, J. Chem. Phys. **126**, 044108 (2007).
[38]M. Yang, F. Yang, K. A. Jackson, and J. Jellinek, J. Chem. Phys. **132**, 064306 (2010).
[39]G. Guzmán-Ramirez, F. Aguilera-Granja, J. Robles, Eur. Phys. J. D **57**, 49 (2010); **57**, 335 (2010).
[40]A. B. Anderson, J. Chem. Phys. **64**, 1744 (1978).
[41]M. Witko and H.-O. Beckmann, Mol. Phys. **47**, 945 (1982).
[42]X. Wang, X. Wan, H. Zhou, S. Takami, M. Kubo, and A. Miyamoto, J. Mol. Struct., Theochem **579**, 221 (2002).
[43]A. Del Vitto, C. Sousa, F. Illas, and G. Pacchioni, J. Chem. Phys. **121**, 7457 (2004).
[44]S. I. Bosko, L. V. Moskaleva, A. V. Matveev, and N. Rösch, J. Phys. Chem. A **111**, 6870 (2007).
[45]M. Huix-Rotllant, A. Deka, A. V. Matveev, S. I. Bosko, L. V. Moskaleva, and N. Rösch, Int. J. Quantum Chem. **108**, 2978 (2008).
[46]Y. Zhou and Z. Zeng, J. Nanosci. Nanotechnol. **10**, 5404 (2010).
[47]S. Lecoultre, A. Rydlo, C. Félix, J. Buttet, S. Gilb, and W. Harbich, J. Chem. Phys. **134**, 074303 (2011).
[48]J. C. Idrobo, S. Öğüt, and J. Jellinek, Phys. Rev. B **72**, 085445 (2005); **77**, 239901 (2008).
[49]S. Öğüt, J. C. Idrobo, J. Jellinek, and J. L. Wang, J. Cluster Sci. **17**, 609 (2006).
[50]J. C. Idrobo, S. Öğüt, K. Nemeth, J. Jellinek, and R. Ferrando, Phys. Rev. B **75**, 233411 (2007).
[51]J. C. Idrobo, W. Walkosz, S. F. Yip, S. Öğüt, J. Wang, and J. Jellinek, Phys. Rev. B **76**, 205422 (2007); **77**, 249903 (2008).
[52]K. Baishya, J. C. Idrobo, S. Öğüt, M. L. Yang, K. Jackson, and J. Jellinek, Phys. Rev. B **78**, 075439 (2008).
[53]M. L. Tiago, J. C. Idrobo, S. Öğüt, J. Jellinek, and J. R. Chelikowsky, Phys. Rev. B **79**, 155419 (2009).
[54]G. Mie, Ann. Phys. (Leipzig) **330**, 377 (1908).
[55]R. Gans, Ann. Phys. (Leipzig) **342**, 881 (1912).
[56]J. C. Idrobo and S. T. Pantelides, Phys. Rev. B **82**, 085420 (2010).
[57]Information about PARSEC can be found at [http://parsec.ices.utexas.edu/].
[58]Y. Zhou, Y. Saad, M. L. Tiago, and J. R. Chelikowsky, Phys. Rev. E **74**, 066704 (2006).
[59]A. G. Shenstone, Philos. Trans. R. Soc. London A **241**, 297 (1948); see also [http://physics.nist.gov/PhysRefData/Handbook/Tables/coppertable3.html].
[60]As noted in Sec. II, our TDLDA computations presented here are for ground state structures of Cu_n clusters as found in Refs. 35 and 36. We have not considered low-energy isomers that are higher in energy by a few tenths of an electronvolt or typically much less as size increases (Refs. 35 and 38). For small sizes,

low-energy isomers can have substantially different absorption spectra compared to those of ground state structures, as revealed in the recent computations of Lecoultre *et al*. (Ref. 47). Based on our work for Ag_n clusters in the intermediate size range ($10 \leqslant n \leqslant 20$) (Ref. 52), we expect the differences between the absorption spectra of ground state and the first few low-energy isomers to be less significant.

[61] J. C. Idrobo, M. Yang, K. A. Jackson, and S. Öğüt, Phys. Rev. B **74**, 153410 (2006).
[62] A. Heilman, M. Quinten, and J. Werner, Eur. Phys. J. B **3**, 455 (1998).
[63] H. Ehrenreich and H. R. Philipp, Phys. Rev. **128**, 1622 (1962).
[64] N. W. Ashcroft and N. D. Mermin, *Solid State Physics* (Holt, Rinehart, and Winston, New York, 1976).